GEOPHYSICAL RESEARCH PAPERS

No. 6

AIR-COUPLED FLEXURAL WAVES IN FLOATING ICE

F. PRESS
M. EWING
A. P. CRARY
S. KATZ
J. OLIVER

November 1950

Distribution of this document is unlimited.

Base Directorate for Geophysical Research
Air Force Cambridge Research Laboratories
Cambridge Massachusetts

GEOPHYSICAL RESEARCH PAPERS

No. 6

AIR-COUPLED FLEXURAL WAVES IN FLOATING ICE

F. PRESS
M. EWING
A. P. CRARY
S. KATZ
J. OLIVER

November 1950

Base Directorate for Geophysical Research
Air Force Cambridge Research Laboratories
Cambridge Massachusetts

FOREWORD

The work described in No. 6 of the Geophysical Research Papers Series was made possible through the participation of the Geophysical Research Directorate of the Air Force Cambridge Research Laboratories with the Lamont Geological Observatory of Columbia University under USAF Contract ac 396.

Co-authors Press, Oliver and Katz of Part I and co-authors Press and Ewing of Part II are affiliated with the Lamont Observatory. Co-author Crary of Part I is a member of the Geophysical Research Directorate.

The authors wish to acknowledge the work of Mrs. Marie Flanagan in computing and plotting the curves of this paper.

ABSTRACT

PART I

Experimental studies of the propagation of elastic waves on floating ice sheets were made on the ice of Lake Superior and Lake Cayuga. Elastic waves were produced by small explosive charges detonated at various depths in the water, within the ice, and in the air. Seismic detectors consisting of a spread of geophones, a microphone, and a hydrophone recorded the resultant wave motion at various distances.

Shots in the water produced the normal sequence of dispersive flexural waves. For shots in the air the dispersive flexural waves were absent and a train of constant frequency waves was observed, beginning gradually at the approximate time $t = r/2v_a$ and culminating with the arrival of the air wave at the time $t = r/v_a$ (r is the range and v_a is the speed of sound in air). These waves were interpreted as air-coupled flexural waves. The frequency of the air-induced waves is that of flexural waves whose phase velocity equals the speed of sound in air. The generated wave train precedes the air disturbance since the group velocity of flexural waves exceeds the phase velocity, all in accordance with classical theory. The frequency of the air-coupled vibration is simply related to the ice thickness.

The interpretation was supported by subsequent tests which consisted of shooting on shore and recording on the ice, shooting and recording on ice sheets of varying thickness, and recording air-coupled flexural vibrations with microphones.

PART II

The exact theory for air-coupled flexural waves in a floating ice sheet is derived for the case of an impulsive point source situated either in the air or in the water beneath the ice.

CONTENTS

AIR-COUPLED FLEXURAL WAVES IN FLOATING ICE *

PART I
EXPERIMENTAL STUDIES OF AIR-COUPLED FLEXURAL WAVES

INTRODUCTION

During a period of three weeks in February and March 1950, experimental studies of the propagation of elastic waves in floating ice sheets were made on Lake Superior and Lake Cayuga. These experiments were designed to study compressional, shear, flexural, and longitudinal surface waves in the ice-water system. In the course of the investigations an air-coupled flexural wave was discovered. Sufficient time remained to firmly establish the existence of this wave by performing additional tests.

The experimental data obtained for air-coupled flexural waves and a brief summary of the theory are given in Part I of this report.

A detailed theoretical investigation of these waves is presented in Part II.

EXPERIMENTAL PROCEDURE

The standard method of seismic refraction measurements was employed in the experiments on Lake Superior and Lake Cayuga. A spread consisting of 8 geophones and 2 horizontal seismometers was placed on the ice surface. Additional data were occasionally obtained from a hydrophone at various depths in the water and a microphone in the air. Shots consisted of blasting caps or ½ lb TNT demolition blocks detonated at various depths in the water, in the ice, and at various heights in the air. The spread interval varied during the course of the experiments, and shot distances ranged up to 7,414 ft. The instant of the explosion was transmitted to the recording truck by wire.

Two types of ice were encountered during the tests. Near shore a rough, hummocky ice sheet was found in which thickness variations of up to 50% were not uncommon along a profile. About a mile off shore a smooth newly formed ice sheet was found. Ice thickness varied 15% or less in the smooth sheet.

*Manuscript received for publication 18 July 1950.

FLEXURAL WAVES

A typical record of flexural waves for a shot consisting of a blasting cap exploded at the under surface of the ice at a spread distance of 4614-5014 ft is shown in Fig. 1a. The ice thickness averaged 1.1 ft and the water depth 126 ft.

Flexural vibrations in a floating ice sheet are essentially surface waves analogous to gravity waves on water, Rayleigh waves on the surface of an elastic solid, or to flexural waves in a rod or thin plate. Ewing and Crary[1] made a detailed investigation of these waves. They derived equations for phase and group velocity as a function of frequency, taking gravity, compressibility of water, and finite water depth into account. Their observations of dispersion of flexural waves on lake ice agreed quite well with the theoretically derived dispersion curves.

An expression for the phase velocity c of flexural waves is easily derived[2] for the case of deep water (neglecting air)

$$c^2 = \frac{(1/3)\pi^2\gamma^2 v_p^2 + (\rho_w/\rho_i)g\lambda/4\pi^2\gamma}{1 + (\rho_w/\rho_i)/2\pi\gamma\sqrt{1 - c^2/v_w^2}} \quad , \tag{1}$$

where γ is the ratio of ice thickness H to wavelength λ, and is related to frequency f by the equation $\gamma = Hf/c$, v_p is the velocity of longitudinal waves in the ice sheet, v_w is the speed of sound in water, g is the gravitational constant, and ρ_w, ρ_i are the densities of water and ice respectively. It can be seen from Eq.(1) that for large wavelengths (γ small), the phase velocity is small, approaching the value $\sqrt{g\lambda/2\pi}$ of gravity waves on deep water. As the wavelength decreases (γ increasing) the phase velocity increases. The gravity term in Eq. (1) can be neglected for wavelengths (or frequencies) for which $\gamma > 0.02$. Group velocity U can be computed as a function of γ from Eq. (1) and the familiar expression

$$U = c + \gamma\, dc/d\gamma \quad . \tag{2}$$

---

[1] Maurice Ewing and A. P. Crary, "Propagation of Elastic Waves in Ice," *Physics*, vol. 5, no. 7, pp 1-10; 1934.

[2] Ibid.

In Fig. 2 dimensionless phase and group velocity curves computed from Eqs. (1) and (2) are plotted against γ for the case $v_p = 11{,}500$ ft/sec, $v_w = 4650$ ft/sec, $\rho_w/\rho_i = 1.0904$. The dispersion observed on the seismogram of Fig. 1a is plotted as Fig. 3. Good agreement with the theoretical group velocity curves for $H = 1.0$-1.1 ft is found. Records of flexural waves illustrated in Fig. 1a were obtained for all shots located either in the ice or in the water. The amplitudes decreased as the depth of the shot increased, waves of higher frequency decreasing more rapidly than those of lower frequency, as one would expect from theory. Dispersion was found to be independent of distance provided shot distances were sufficiently large for the dispersion pattern to develop (> 500 ft).

AIR-COUPLED FLEXURAL WAVES

A pronounced change in record character was observed for shots fired on or above the ice surface. Figure 1b is the seismogram of a shot of ½ lb exploded in air 17 inches above the surface of the ice at the same location as the water shot illustrated in Fig. 1a. Both records are aligned with respect to time after the shot instant. Flexural vibrations from the water shot are characterized by a long dispersive train beginning with waves of frequency 75 c/s and velocity about 2150 ft/sec and ending gradually with waves having a frequency of 8 c/s and velocity about 650 ft/sec. The air shot consists almost entirely of a train of constant frequency vibrations the first waves of which travel with a velocity of about 2000 ft/sec. A gradual increase of amplitude with time is observed (although some grouping tends to occur). The constant frequency waves build up until the arrival of a pulse (indicated by arrows), after which the amplitudes diminish rapidly.

Figure 4, a seismogram, recorded at reduced gain, of an air shot of ½ lb detonated 1 ft above the ice at a spread distance of 6114-6514 ft, clearly shows the nature of this pulse (indicated by arrows). It consists of a single cycle wave travelling with the speed of sound in air. There is little activity in the air shot after the arrival of the air wave, whereas in the water shot, flexural vibrations continue to arrive after the time corresponding to that of the air wave.

Except for minor changes, the general characteristics of the records in Fig. 1a were observed for all shots within the ice or in the water near the ice bottom. All air shots produced records similar to the seismograms of Figs. 1b and 4.

The constant frequency train of waves culminating with the arrival of the air wave is interpreted as an air-coupled flexural wave.

A simple yet general explanation of the main characteristics of air-coupled surface

waves can be given with the aid of the classical theory of travelling disturbances.[3,4,5] If the reaction of the surface wave on the air is neglected, the air wave can be treated as a pressure pulse travelling over the surface of a dispersive medium with velocity v_a. We can think of the air wave as imparting a succession of impulses at infinitesimally small, equal intervals of time as it moves over the surface. Each impulse produces a dispersive train of waves. Superposition of the successive wave systems results in reinforcement only for those waves whose phase velocity is equal to the velocity v_a of the air pulse. The waves thus produced have a discrete frequency which can be obtained from the phase velocity curve of the dispersive medium from the value γ_a corresponding to $c = v_a$ (Fig. 2). Since waves of a given frequency propagate with the group velocity associated with that frequency, the induced constant frequency surface wave will precede or follow the air wave according as $U > c$ or $U < c$. Group velocity exceeds phase velocity for flexural waves, and accordingly an air shot can be expected to produce a train of constant frequency waves ending abruptly with the air wave. Air-coupled gravity waves and surface elastic waves would follow the arrival of the air wave.

Possible existence of air-coupled Rayleigh waves was discussed briefly in Bateman.[6]

If the air-ice-water system is treated as a single acoustic unit, one can derive phase and group velocity curves analogous to those presented in Fig. 2. N. Haskell[7] derived such curves for the steady state. Identical curves were derived by Press and Ewing in a subsequent investigation of the exact theory of air-coupled flexural waves originating in an impulsive point source (Part II, Fig. 9 (note that $v_1 = v_a$)). A striking feature of these curves is the extreme steepness in the group velocity at γ_a. Since the predominant waves observed at a distant point are those whose frequency and velocity are determined by the group velocity curve,[8] we can expect a train of waves of constant frequency $f_a = \gamma_a v_a / H$ beginning at a time $r = r/2.2v_a$ and continuing until the time $t = r/v_a$. Calculation of the excitation function for these waves (Part II) indicates that in an air shot they will predominate over waves whose travel time and frequency are determined from

---

[3] H. Lamb, "On Waves Due to a Travelling Disturbance with an Application to Waves in Superposed Fluids," *Phil. Mag.*, vol. 31, no. 6, p 387; 1916.

[4] H. Lamb, "On Wave Patterns Due to a Travelling Disturbance," *Phil. Mag.*, vol. 31, no 6, p 539; 1916.

[5] H. Lamb, "Hydrodynamics," Cambridge University Press, 6th Ed., 1932: pp 413-415.

[6] H. Bateman, "Rayleigh Waves," *National Academy of Science Proceedings*, vol. 24, pp 315-320; 1938.

[7] N. Haskell, personal communication; March 10, 1950.

[8] See, for example, T. H. Havelock, "The Propagation of Disturbances in Dispersive Media," *Cambridge Tracts in Mathematical Physics*, no. 17, Cambridge University Press; 1914.

the remaining portions of the group velocity curve. For an ice or water shot the complete theory indicates that the constant frequency waves are vanishingly small and waves following the part of the group velocity curve to the left of the maximum predominate. It should be noted that the dispersion in these waves for frequency $f < f_a$ is almost identical to that obtained from the group velocity curve of Fig. 2, which was calculated under the assumption that air had negligible effect on flexural waves. Thus it is only for an air shot that waves propagated according to the steep portion of the group velocity curve would be observed. It is these waves which we call air-coupled flexural waves.

The frequency of air-coupled flexural waves depends only on the parameter γ_a, the ice thickness, and the velocity of sound in air. The value of γ_a depends on the elastic constants of the ice, in accordance with Eq. (1). For smooth ice on Lake Superior $\gamma_a = 0.091$, and taking $v_a = 1070$ ft/sec, we can write the following simple equation for frequency in terms of ice thickness H (measured in feet):

$$f_a = 97/H \quad . \tag{3}$$

Values of γ_a as a function of v_p have been computed, assuming the same constant values for the other parameters of Eq. (1) used earlier. The results of these calculations, plotted in Fig. 5, can be used to obtain γ_a correct to within a few percent.

On the smooth ice of Lake Superior the observed frequency f_a (Figs. 1b and 3) averaged about 78 c/s. Ice thickness sampled at 5 locations along the profile gave an average value of 1.1 ft, and the theoretically expected frequency calculated for this value from Eq. (3) is 88 c/s, giving reasonably good agreement, in view of the uncertainty of the measured value of H.

Records obtained on Lake Cayuga gave a frequency of 150 c/s for the air-coupled flexural vibrations. Figure 6 illustrates a shot in which a cap was detonated at a depth of 1 inch in ice approximately 8 inches thick. Water depth was 4.3 ft and a spread of 500-710 ft was used. Since $v_p = 10{,}200$ ft/sec on the Lake Cayuga ice, $\gamma_a = 0.097$ and we can write the following equation for frequency:

$$f_a = 104/H \quad . \tag{4}$$

Since $H = 0.66$ ft, $f_a = 158$ c/s. Agreement with the observed value is good despite the fact that shallow water underlay the ice and that Eq. (4) is based on deep water theory. The train of dispersive, long-period, flexural waves which follows the air wave on the Lake Cayuga air-shot is probably due to the fact that the shot was partly in the ice, thus

exciting both air-coupled waves and ordinary flexural waves.

Records of flexural waves from both water and air shots were obtained for propagation paths across rough ice in which the ice thickness varied greatly. The flexural vibrations from a water shot in rough ice exhibited the characteristic dispersion although the waves were more irregular and amplitude variations were more pronounced. An air shot across rough ice produced the seismogram, shown in Fig. 7. In this shot, a ½ lb charge was detonated on the surface of the ice at an approximate distance of 4000 ft from the nearest geophone. A predominant frequency averaging 68 ± 3 c/s is observed for the air-coupled waves. Since the elastic constants of rough ice are slightly different from those of smooth ice the value of γ_a for the two media will differ. For longitudinal waves in rough ice we take the observed value $v_p = 10{,}000$ ft/sec. Using the same values for ρ_w, ρ_i, ρ_a, v_w, v_a as before, we find $\gamma_a = 0.099$, which gives for the rough ice

$$f_a = 106/H \quad . \tag{5}$$

Thickness of the rough ice measured at eight locations varied from 1.1 to 2.1 ft and averaged 1.7 ft. Computing the theoretical frequency from Eq. (5) gives 62 c/s, in good agreement with the observed value of 68 c/s.

Air-coupled flexural vibrations in rough ice show characteristics similar to those observed for shots in smooth ice. Wave amplitudes build up as the time for the arrival of the air wave is approached. However, the air wave does not arrive as a distinct pulse as is the usual case for smooth ice and some low frequency activity continues after the air wave. Only the microphone trace, in Fig. 7, registers the exact instant of the passage of the air pulse. Scattering, air-wave echoes, variations in group velocity--all due to irregularities in ice thickness--are believed to be responsible for these differences on the records obtained in rough ice. A striking feature of the seismogram in Fig. 7 is the recording of a portion of the constant frequency wave train by a microphone located approximately 1 ft above the ice. Records have been obtained in which microphones have registered even larger portions of air-coupled vibrations. This is indeed confirmation of coupling between ice and air.

As an additional test, a ½ lb charge was detonated in a tree on shore at a distance of 20 ft from the edge of the ice sheet and at a height of 20 ft above the ice surface. Unlike the usual air shot records the seismogram obtained showed no longitudinal ice wave or compressional water wave. However, the air-coupled flexural waves were almost indistinguishable from those obtained for shot points over ice.

In several water shots for shot depths ranging from 0 to 50 ft beneath the bottom of the ice, a brief, faint, yet definite train of air-coupled waves is observed riding on the

larger amplitude flexural waves. Since the shallow shots blow out, (i.e., the gas bubble breaks out and partially explodes in the air) a partial air wave is set up, inducing a coupled vibration. For the deeper shots which do not blow out it is tentatively suggested that some sound energy enters the air over the shot point by diffraction. Aided by a favorable air velocity gradient, this energy induces a coupled vibration.

PART II
THEORY OF AIR-COUPLED FLEXURAL WAVES

INTRODUCTION

In the course of a study of the phenomena associated with the famous explosion of the volcano Krakatoa[9,10] in the Straits of Sunda, the authors noted a simultaneous arrival of an air wave and tidal disturbance at several widely separated locations. While this curious phenomenon had been noticed previously,[11] it had been passed off as a coincidence; the tidal waves were attributed to non-related earthquakes. It is now the belief of the authors that the simultaneous arrival of an air wave and tidal disturbance resulted from coupling between the atmospheric pressure wave and the ocean.

It is surprising at first to think of coupling between the atmosphere and the ocean especially since the density contrast between the two media is so great. It can be generally shown, however, that coupling between air waves and surface waves of all types is appreciable when the phase velocity of the surface wave is very close to the speed of sound in air.

The existence of air-coupled surface waves was firmly established in the experimental studies reported in Part I of this paper. A general explanation of these waves was given on pages 7 and 8 of that part.

In Part II the exact theory for air-coupled flexural waves in a floating ice sheet is derived for the case of an impulsive point source situated either in the air or in the water beneath the ice.

A complete discussion of the theory of air-coupled gravity waves, with application to the explosion of Krakatoa, is reserved for another paper.

---

[9] G. J. Symond, *The Eruption of Krakatoa and Subsequent Phenomena*, Trübner & Co., London; 1888.

[10] C. L. Pekeris, "The Propagation of a Pulse in the Atmosphere," *Proc. Roy. Soc.*, vol. A171, p 434; 1939.

[11] R. D. M. Verbeek, Krakatau, Batavia; 1886.

THE THEORY

Consider the propagation of flexural waves in a plate of infinite extent floating on deep water, the thickness of the plate H being small compared to wavelengths considered. Overlying the plate is an infinite atmosphere having density ρ_1, and sound velocity v_1. The plate has volume density ρ_2, longitudinal wave velocity v_p; the water has density ρ_3, sound velocity v_3. A Cartesian coordinate system is chosen with the x, y axes in the equilibrium plane of the plate and the z axis vertically upward. We will use the coordinates z and $r = \sqrt{x^2 + y^2}$ and denote the corresponding displacements by w and q. The subscripts 1, 2, 3 hereafter refer to the air, plate, and water respectively.

SIMPLE HARMONIC POINT SOURCE IN AIR

We wish to determine the vertical displacement w of the plate due to the passage of a system of flexural waves which originate in a point source of sound waves at $r = 0$ and $z = d$. Particular interest is in the solutions which predominate at large distances from the source. Assuming simple harmonic motion $\exp(-i\omega t)$ we introduce the velocity potentials ϕ_1 and ϕ_3 from which the component velocities $\dot{q}$ and $\dot{w}$ and the pressure p can be obtained as follows:

$$\left.\begin{aligned} p_i &= \rho_i \partial\phi_i/\partial t \\ \dot{q}_i &= \partial\phi_i/\partial r \qquad i = 1, 3 \\ \dot{w}_i &= \partial\phi_i/\partial z \quad . \end{aligned}\right\} \tag{6}$$

It is convenient to divide the air into two regions by the plane $z = d$ and to denote values of velocity potential etc. for the region $0 < z < d$ by primed symbols.

It is required that the functions ϕ be solutions of the wave equation:

$$v_i^2 \nabla^2 \phi_i = \partial^2\phi_i/\partial t^2 \quad , \qquad i = 1, 3 \tag{7}$$

where

$$\nabla^2 = \partial^2/\partial r^2 + (1/r)\partial/\partial r + \partial^2/\partial z^2 \quad .$$

Solutions of Eq. (7) must satisfy the boundary conditions (for a thin plate)

$$\partial\phi_1'/\partial z = \partial w_2/\partial t = \partial\phi_3/\partial z \qquad \text{at} \quad z = 0 \tag{8}$$

and w_2 satisfies the equation for flexural vibrations of the plate[12]

$$H\rho_2\partial^2 w_2/\partial t^2 = -(H^3\rho_2 v_p^2/12)\nabla^4 w_2 - \rho_3 g w_2 - \rho_3\partial\phi_3/\partial t + \rho_1\partial\phi_1'/\partial t \quad , \tag{9}$$

where v_p is the velocity of longitudinal waves in the plate, g is the gravitational acceleration, and

$$\nabla^4 = \frac{1}{r}\frac{\partial}{\partial r}\left[r\frac{\partial}{\partial r}\left\{\frac{1}{r}\frac{\partial}{\partial r}\left[r\frac{\partial}{\partial r}\right]\right\}\right] \quad .$$

Equation (9) is derived under the assumption that Poisson's constant for the plate has the value 0.25.

We use a method of representing a simple harmonic point source originally given by Lamb.[13] The procedure is first to obtain the solutions to the problem where a periodic pressure is applied to the entire plane $z = d$ symmetrically about the z axis and then to pass to the case of a point source utilizing the Fourier-Bessel integral. A point source located at $r = 0$, $z = d$ is represented by ultimately requiring continuity of pressure in the plane $z = d$ and continuity of vertical velocity everywhere in the same plane except at the source where the air above and below the source moves in opposite directions. Here the discontinuity in vertical velocity is proportional to a function $F(r)$ which vanishes everywhere except at $r = 0$ where it becomes infinite in such a manner that its integral over the plane $z = d$ is finite.

Typical solutions of Eq. (7) are of the form:

$$\phi_1 = A\exp(-\eta z)J_0(kr)\exp(-i\omega t) \qquad z > d \tag{10}$$

---

[12] Maurice Ewing and A. P. Crary, "Propagation of Elastic Waves in Ice," *Physics*, vol. 5, part II, no. 6, pp 1-10; 1934.

[13] H. Lamb, "On the Propagation of Tremors over the Surface of an Elastic Solid," *Phil. Trans. Roy. Soc. Lond.*, Ser. A, vol. 203, pp 1-42; 1904.

$$\phi_1' = [B \exp(\eta z) + C \exp(-\eta z)] J_0(kr) \exp(-\iota\omega t) \qquad 0 < z < d \qquad (11)$$

$$\phi_3 = E \exp(\zeta z) J_0(kr) \exp(-\iota\omega t) \quad , \qquad z < 0 \qquad (12)$$

Flexural motion of the plate is given by:

$$w_2 = D J_0(kr) \exp(-\iota\omega t) \quad . \qquad (13)$$

The separation constants η, ζ obtained by substituting Eqs. (10), (11), and (12) in Eq. (7) are

$$\eta^2 = k^2 - \omega^2/v_1^2 \quad , \qquad \zeta^2 = k^2 - \omega^2/v_3^2 \quad , \qquad (14)$$

and are defined as positive real or positive imaginary.

These solutions must satisfy two additional boundary conditions at the plane $z = d$ where the pressure is continuous,

$$\rho_1 \partial\phi_1/\partial t = \rho_1 \partial\phi_1'/\partial t \quad , \qquad (15)$$

and the vertical velocity is discontinuous,

$$\partial\phi_1/\partial z - \partial\phi_1'/\partial z = 2\dot{Y} J_0(kr) \exp(-i\omega t) \quad . \qquad (16)$$

the air above and below the plane moving in opposite directions.

The expression for ϕ_1' is a general form. ϕ_1 and ϕ_3 have been chosen to decrease exponentially with distance from the plate since we are particularly interested in solutions for which there is no radiation from the plate into the surrounding media.

Five simultaneous linear equations result when Eqs. (10) through (13), the solutions of Eq. (7), are substituted in Eqs. (8), (9), (15), and (16), the boundary conditions. Solving for A, B, C, D, E from these equations gives·

$$A = \frac{-\dot{Y}}{\eta G(k)} [g(k) \exp(-\eta d) + G(k) \exp(\eta d)] \qquad (17)$$

$$B = \frac{-Y}{\eta}[\exp(-\eta d)] \tag{18}$$

$$C = \frac{-Y}{\eta G(k)}[g(k)\exp(-\eta d)] \tag{19}$$

$$D = \frac{-2Y}{\eta G(k)}[(\rho_1/\rho_2)\eta\zeta i\omega\exp(-\eta d)] \tag{20}$$

$$E = \frac{-2Y}{\eta G(k)}[(\rho_1/\rho_2)\omega^2\eta\exp(-\eta d)] \quad , \tag{21}$$

where

$$G(k) = (\rho_3/\rho_2)\omega^2\eta + \eta\zeta(H\omega^2 - H^3v_p^2k^4/12 - g\rho_3/\rho_2) + (\rho_1/\rho_2)\omega^2\zeta \quad , \tag{22}$$

$$g(k) = (\rho_3/\rho_2)\omega^2\eta + \eta\zeta(H\omega^2 - H^3v_p^2k^4/12 - g\rho_3/\rho_2) - (\rho_1/\rho_2)\omega^2\zeta \quad . \tag{23}$$

We now generalize the discontinuity of vertical velocity in the plane $z = d$ by means of the Fourier-Bessel integral

$$F(r) = \int_0^\infty J_0(kr)k\,dk\int_0^\infty F(\lambda)J_0(k\lambda)\lambda\,d\lambda \quad . \tag{24}$$

$F(\lambda)$ is chosen to vanish for all but infinitesimal values of λ in such a manner that

$$\int_0^\infty F(\lambda)2\pi\lambda\,d\lambda$$

has a finite constant value. Thus taking $Y = k\,dk$ in the Eqs. (10) through (13) and (17) through (21) and integrating with respect to k from 0 to ∞, we obtain solutions which satisfy the appropriate conditions at $z = 0$ and meet the additional requirements for a point source, namely continuity of pressure in the plane $z = d$ and continuity of vertical

particle velocity everywhere in this plane except at the source $r = 0$ where a discontinuity in $\partial\phi/\partial z$ exists proportional to

$$F(r) = \int_0^\infty J_0(kr)k\,dk$$

which becomes infinite in such a way that its integral over the plane $z = d$ is finite.

The solution for a periodic point source is therefore

$$w_2 = -\exp(-\imath\omega t)\int_0^\infty J_0(kr)k\,dk\left\{2(\rho_1/\rho_2)\imath\omega\zeta\,\exp(-\eta d)/G(k)\right\} . \qquad (25)$$

Following the procedure of Lamb,[14] Sezawa,[15] and Pekeris,[16] Eq. (25) will be evaluated by integration along suitable contours in the complex plane $Z = k + im$. Let

$$E(Z) = -(\rho_1/\rho_2)(Z^2 - \omega^2/v_3^2)^{1/2}i\omega\exp\left[-d(Z^2 - \omega^2/v_1^2)^{1/2}\right] ,$$

and consider the two integrals whose sum can be used to evaluate the integral in Eq. (25):

$$\int_c H_0'(Zr)[E(Z)/G(Z)]Z\,dZ \qquad (26)$$

and

$$\int_{c'} H_0^2(Zr)[E(Z)/G(Z)]Z\,dZ . \qquad (27)$$

---

[14] H. Lamb, "On the Propagation of Tremors over the Surface of an Elastic Solid," *Phil. Trans. Roy. Soc. Lond.*, Ser. A, vol. 203, pp 1-42; 1904.

[15] K. Sezawa, "Love Waves Generated from a Source of a Certain Depth," *Bull. Earth. Res. Inst. Tokyo*, vol. 13, no. 1, pp 1-17; 1935.

[16] C. L. Pekeris, "Theory of Propagation of Explosive Sound in Shallow Water," *Geol. Soc. Amer.*, Mem. 27, Propagation of Sound in The Ocean; 1948.

Integrals (26) and (27) are taken around paths C and C' in the first and fourth quadrants respectively (Fig. 8). $G(Z)$ is obtained from Eq. (22). Integral (26) has branch points at $Z = \omega/v_1$ and $Z = \omega/v_3$ and a pole at $Z = k_n$ which is the root of $G(Z) = 0$. $G(k_n) = 0$ is the characteristic, or frequency equation for air-coupled flexural waves on a floating ice sheet. Integral (27) has neither branch points nor poles. That the singular points lie in the first quadrant only can be demonstrated[17] by temporarily including small frictional forces in the original equations of motion. We denote by η' , $\pm\zeta'$ the values assumed by η , ζ on both sides of the line $k = \omega/v_3$, and, by $\pm\eta''$, ζ'' the values on the two sides of $k = \omega/v_1$ (Fig. 8). For small values of m we can write:

$$\eta' = i(\omega^2/v_1^2 - \omega^2/v_3^2)^{1/2} , \qquad \eta'' = (2m\omega/v_1)^{1/2}\exp(i\pi/4)$$

$$\zeta' = (2m\omega/v_3)^{1/2}\exp(i\pi/4) , \qquad \zeta'' = (\omega^2/v_1^2 - \omega^2/v_3^2)^{1/2} .$$

Taking Integral (26) around the indicated contours and letting the radius of the circular arc approach infinity, we find:

$$\int_0^\infty H_0'(kr)[E(k)/G(k)]k\,dk + \int_0^\infty H_0'(Z''r)Z''\,dm(\rho_1/\rho_2)\omega\zeta''\left\{\frac{\exp(-\eta''d)}{(\rho_3/\rho_2)\omega^2\eta'' + \eta''\zeta''[H\omega^2 - H^3v_p^2Z''^4/12 - g(\rho_3/\rho_2)] + (\rho_1/\rho_2)\omega^2\zeta''}\right.$$

$$\left. - \frac{\exp(\eta''d)}{-(\rho_3/\rho_2)\omega^2\eta'' - \eta''\zeta''(H\omega^2 - H^3v_p^2Z''^4/12 - g\rho_3/\rho_2) + (\rho_1/\rho_2)\omega^2\zeta''}\right\} + \int_0^\infty H_0'(Z'r)Z'\,dm(\rho_1/\rho_2)\omega\exp(-\eta'd)\times$$

$$\left\{\frac{\zeta'}{(\rho_3/\rho_2)\omega^2\eta' + \eta'\zeta'(H\omega^2 - H^3v_p^2Z'^4/12 - g\rho_3/\rho_2) + (\rho_1/\rho_2)\omega^2\zeta'} + \frac{\zeta'}{(\rho_3/\rho_2)\omega^2\eta' - \eta'\zeta'(H\omega^2 - H^3v_p^2Z'^4/12 - g\rho_3/\rho_2) - (\rho_1/\rho_2)\omega^2\zeta'}\right\}$$

$$-\int_\omega^0 \frac{H_0'(imr)m\,dm(\rho_1/\rho_2)\omega(m^2+\omega^2/v_3^2)^{1/2}\exp[-id(m^2+\omega^2/v_1^2)^{1/2}]}{i(\rho_3/\rho_2)\omega^2(m^2+\omega^2/v_1^2)^{1/2} - (m^2+\omega^2/v_1^2)^{1/2}(m^2+\omega^2/v_3^2)^{1/2}(H\omega^2 - H^3v_p^2m^4/12 - g\rho_3/\rho_2) + i(\rho_1/\rho_2)\omega^2(m^2+\omega^2/v_3^2)^{1/2}}$$

$$- 2\pi i\frac{H_0'(k_nr)k_nE(k_n)}{\partial G(k_n)/\partial k} = 0 , \qquad (28)$$

where k_n is the root of $G(k) = 0$ and $Z' = \omega/v_3 + im$ and $Z'' = \omega/v_1 + im$ respectively in the second and third integrals of Eq. (28). Integrating (27) around the contour in the fourth quadrant gives:

[17] K. Sezawa, "Love Waves Generated from a Source of a Certain Depth," *Bull. Earth. Res. Inst. Tokyo*, vol. 13, no. 1, pp 1-17; 1935.

$$\int_0^{\infty} H_0^2(kr)\,\frac{E(k)}{G(k)}\,k\,dk$$

$$-\int_{-\infty}^{0} \frac{H_0^2(\imath mr)\,m\,dm(\rho_1/\rho_2)\,\omega\,(m^2+\omega^2/v_3^2)^{1/2}\exp[-\imath d(m^2+\omega^2/v_1^2)^{1/2}]}{\imath(\rho_3/\rho_2)\,\omega^2(m^2+\omega^2/v_1^2)^{1/2}-(m^2+\omega^2/v_1^2)^{1/2}(m^2+\omega^2/v_3^2)^{1/2}(H\omega^2-H^3v_p^2m^4/12-g\beta/\rho_2)+\imath(\rho_1/\rho_2)\,\omega^2(m^2+\omega^2/v_3^2)^{1/2}}$$

$$= 0\,. \qquad (29)$$

The integrals along the infinite arcs in the first and fourth quadrants vanish because of the well known properties of the Hankel functions. From the relation $H_0^1(im) = -H_0^2(-im)$ it can be seen that the last integrals of Eqs. (28) and (29) are equal and opposite in sign. Since $2J_0(kr) = H_0^1(kr) + H_0^2(kr)$, the sum of the first integrals in Eqs. (28) and (29) is equivalent to Eq. (25). Using the expansions $H_0^1(x) \rightarrow \exp[i(x-\pi/4)]/(\pi x/2)^{1/2}$ and $H_0^2(x) \rightarrow \exp[-i(x-\pi/4)]/(\pi x/2)^{1/2}$, we add Eqs. (28) and (29) and obtain for large values of r

$$w_2 = w_0 + w' + w'' \quad , \qquad (30)$$

where w_0 represents the residue:

$$w_0 = 2\pi i\,\frac{k_n E(k_n)\exp[i(k_n r-\omega t-\pi/4)]}{(\pi k_n r/2)^{1/2}\,\partial G(k_n)/\partial k} \quad , \qquad (31)$$

and w' and w'' are the two branch line integrals:

$$w' = \frac{-2\exp[i(r\omega/v_3-\omega t-\pi/4)]}{(\pi/2)^{1/2}}\int_0^{\infty}\frac{\exp(-mr)}{(Z'r)^{1/2}}\,Z'\,dm(\rho_1/\rho_2)\,\omega\,\exp(-\eta' d)\;\times$$

$$\left\{\frac{(\rho_3/\rho_2)\omega^2\eta'\zeta'}{[(\rho_3/\rho_2)\omega^2\eta']^2-[\eta'\zeta'(H\omega^2-H^3v_p^2Z'^4/12-g\rho_3/\rho_2)+(\rho_1/\rho_2)\omega^2\zeta']^2}\right\} \qquad (32)$$

$$w'' = \frac{2\exp[i(r\omega/v_1-\omega t-\pi/4)]}{(\pi/2)^{1/2}}\int_0^{\infty}\frac{\exp(-mr)}{(Z''r)^{1/2}}\,Z''dm(\rho_1/\rho_2)\,\omega\zeta''\;\times$$

$$\left\{\frac{\cosh(\eta'' d)[(\rho_3/\rho_2)\omega^2-\eta''(H\omega^2-H^3v_p^2Z''^4/12-g\rho_3/\rho_2)]+\sinh(\eta'' d)(\rho_1/\rho_2)\omega^2\zeta''}{-[(\rho_3/\rho_2)\omega^2-\eta''(H\omega^2-H^3v_p^2k''^4/12-g\rho_3/\rho_2)]^2+[(\rho_1/\rho_2)\omega^2\zeta'']^2}\right\}, \qquad (33)$$

where $Z' = \omega/v_3 + i\varepsilon$ in Eq. (32) and $Z'' = \omega/v_1 + i\varepsilon$ in Eq. (33). These definite integrals can be expanded in asymptotic forms by means of the following formula which is readily derived from the integral representation of the gamma function:

$$\int_0^\infty \varepsilon^{1/2}\,\psi(\varepsilon)\,\exp(-\varepsilon r)\,d\varepsilon \;=\; \frac{\Gamma(3/2)}{r^{3/2}}\,\psi(0) + \frac{\Gamma(5/2)}{r^{5/2}}\,\frac{\psi'(0)}{1!} + \cdots \quad . \tag{34}$$

For large r we have:

$$w' \;\to\; \frac{2i(\rho_1/\rho_3)\,\exp[i(r\omega/v_3 - \omega t)]\,\exp[-id(\omega^2/v_1^2 - \omega^2/v_3^2)^{1/2}]}{r^2\,\omega\,(v_3^2/v_1^2 - 1)^{1/2}} \tag{35}$$

$$w'' \;\to\; \frac{2\,\exp[i(r\omega/v_1 - \omega t)]}{r^2 v_1}\left\{\frac{\rho_3/\rho_1}{(\omega^2/v_1^2 - \omega^2/v_3^2)^{1/2}} + (\rho_2/\rho_1)\,[H - H^3 v_\rho^2\omega^2/12v_1^4 - g(\rho_3/\rho_2)/\omega^2] + d\right\} . \tag{36}$$

The solutions given by Eqs. (30) through (36) and (35) through (36) have been expressed as a residue and two integrals along branch lines. The branch line integrals represent waves which travel with velocities v_3 and v_1 and diminish rapidly for large ranges as r^{-2}. The residue represents a train of dispersive waves, whose frequency equation is given by:

$$G(k_n) \;=\; 0 \quad . \tag{37}$$

Since these waves diminish in amplitude as $r^{-1/2}$ they represent the predominant disturbance at large ranges. Using the expression for phase velocity $c = \omega/k$ we can rewrite Eq. (31) in a form more convenient for computation:

$$w_0 \;=\; \frac{W(k_n)}{r^{1/2} v_\rho H^{1/2}} \exp[-dk_n(1 - c^2/v_1^2)^{1/2}]\,\exp[i(k_n r - \omega t - \pi/4)] \quad , \tag{38}$$

where

$$W(k) \;=\; \frac{2(2\pi)^{1/2}(\rho_1/\rho_2)\,(kH)^{1/2}(c/v_\rho)(1 - c^2/v_3^2)^{1/2}}{\{\;\}} \tag{39}$$

$$\{\} = \left\{\frac{(\rho_3/\rho_2)c^2/v_p^2}{(1 - c^2/v_1^2)^{1/2}} + \left[\frac{(1 - c^2/v_1^2)^{1/2}}{(1 - c^2/v_3^2)^{1/2}} + \frac{(1 - c^2/v_3^2)^{1/2}}{(1 - c^2/v_1^2)^{1/2}}\right]\left[kH\,c^2/v_p^2 - (kH)^3/12\right.\right.$$

$$\left.\left. - (\rho_3/\rho_2)(g/k)/v_p^2\right] - (1 - c^2/v_1^2)^{1/2}(1 - c^2/v_3^2)^{1/2}(kH)^3/3 + \frac{(\rho_1/\rho_2)c^2/v_p^2}{(1 - c^2/v_3^2)^{1/2}}\right\} \quad . \tag{40}$$

Equation (37) likewise may be rewritten as:

$$(\rho_3/\rho_2)(c^2/v_p^2)(1 - c^2/v_1^2)^{1/2} + (1 - c^2/v_1^2)^{1/2}(1 - c^2/v_3^2)^{1/2}[kH\,c^2/v_p^2 - (kH)^3/12 - (\rho_3/\rho_2)(g/k)/v_p^2$$

$$+ (\rho_1/\rho_2)(c^2/v_p^2)(1 - c^2/v_3^2)^{1/2} = 0 \quad . \tag{41}$$

Equation (41) is a cubic in kH with the elastic constants of the system as parameters. It defines an implicit relationship between the frequency $f = ck/2\pi$ and the phase velocity c of waves given by Eq. (38). For $c \leq v_1 < v_3$, real values of kH exist. These are plotted in Fig. 9 as a function of the dimensionless parameter $\gamma = kH/2\pi$ for the case $v_1 = 1070$ ft/sec, $v_p = 11,500$ ft/sec, $v_3 = 4650$ ft/sec, $\rho_1/\rho_2 = 0.00141$, $\rho_3/\rho_2 = 1.0904$. The factor $W(k)$ shows the dependence of amplitude upon frequency. The exponential term in Eq. (38) shows the influence of the height of the source on amplitudes. It is seen that wave amplitudes decrease exponentially as $-dk_n(1 - c^2/v_1^2)^{1/2}$.

GENERALIZATION FOR AN ARBITRARY PULSE

In a dispersive system, such as the one under discussion, energy associated with each wavelength or frequency is known to propagate with the group velocity given by the familiar expression:

$$U = c + k\,dc/dk \quad . \tag{42}$$

Carrying out the indicated differentiation, using the functional relationship between c and kH given by Eq. (41), enables one to compute values of U which are plotted in dimensionless form in Fig. 9.

Having obtained the steady state solution for a simple harmonic point source in the air, we proceed to the case of an arbitrary initial disturbance. If the time variation of the initial disturbance at the source is $f(t)$ represented by its Fourier Transform

$$g(\omega) = \int_{-\infty}^{\infty} \exp(i\omega t) f(t)\,dt \quad , \tag{43}$$

then

$$f(t) = (1/2\pi)\int_{-\infty}^{\infty} \exp(-i\omega t) g(\omega)\, d\omega \quad , \tag{44}$$

and the displacement w_0 becomes:

$$w_0 = r^{-1/2} H^{-1/2} (2\pi v_p)^{-1} \int_{-\infty}^{\infty} g(\omega) W(k_n) \exp[-dk_n (1 - c^2/v_1^2)^{1/2}] \exp[i(k_n r - \omega t - \pi/4)]\, d\omega \quad . \tag{45}$$

In Eq. (45), k_n is a function of ω, through Eq. (41). We follow Pekeris in representing the initial disturbance created in an explosion as follows:

$$\left.\begin{aligned} f(t) &= \exp(-\sigma t) \qquad t > 0 \\ &= 0 \quad . \qquad t < 0 \end{aligned}\right\} \tag{46}$$

With this definition we can write

$$f(t) = (1/2\pi)\int_{-\infty}^{\infty} (\sigma - i\omega)^{-1} \exp(-i\omega t)\, d\omega \quad , \qquad g(\omega) = (\sigma - i\omega)^{-1}, \tag{47}$$

$$w_0 = r^{-1/2} H^{-1/2} (2\pi v_p)^{-1} \int_{-\infty}^{\infty} (\sigma - i\omega)^{-1} W(k_n) \exp[-dk_n (1 - c^2/v_1^2)^{1/2}] \exp[i(k_n r - \omega t - \pi/4)]\, d\omega \quad . \tag{48}$$

To evaluate this integral we use Kelvin's approximate method of stationary phase. For a discussion of this method, and the validity of the approximations used the reader is referred to papers by Havelock,[18] Pekeris,[19] and Eckart.[20] Integrating Eq. (48) by the method of stationary phase gives:

$$w_0 = \frac{W(k_0) \exp[-dk_0 (1 - c^2/v_1^2)^{1/2}] \exp[i(k_0 r - \omega_0 t - \pi/4 \pm \pi/4)]}{r H (v_p/v_1)(\sigma - i\omega_0)[(v_1/c)(v_1/U)^2 d(U/v_1)/d\gamma]^{1/2}} , \tag{49}$$

---

[18] T. H. Havelock, "The Propagation of Disturbances in Dispersive Media," *Cambridge Tracts in Mathematical Physics*, No. 17, Cambridge University Press; 1914.

[19] C. L. Pekeris, "Theory of Propagation of Explosive Sound in Shallow Water," *Geol. Soc. Amer.*, Mem. 27, Propagation of Sound in The Ocean; 1948.

[20] Carl Eckart, "Approximate Solution of One Dimensional Wave Equation," *Rev. Mod. Phys.*, vol. 20, no. 2, pp 399-417; 1948.

where the upper or lower sign in the exponential term is to be taken according as $d(U/v_1)/d\gamma$ is negative or positive, and k_0, ω_0, U/v_1 $d(U/v_1)/d\gamma$ are evaluated from the phase and group curve for values of r and t which satisfy $r/t = U$. The approximation used to derive Eq. (49) is valid provided r is large and t is sufficiently removed from stationary values of group velocity. To complete the solution we add to Eq. (49) its complex conjugate since there are two stationary points $\pm\omega_0$ (a solution to Eq. (48) except for a reversal of sign of the phase of the exponential term would have been obtained had we assumed initially a time factor $\exp(i\omega t)$ instead of $\exp(-i\omega t)$). Thus we obtain:

$$w_0 = \frac{2W(k_0)\exp[-dk_0(1-c^2/v_1^2)^{1/2}]\cos(k_0 r - \omega t + \tan^{-1}\omega/\sigma)}{rH(v_p/v_1)(\sigma^2+\omega^2)^{1/2}[(v_1/c)(v_1/U)^2 d(U/v_1)/d\gamma]^{1/2}} \tag{50}$$

for $d(U/v_1)/d\gamma < 0$

$$w_0 = \frac{2W(k_0)\exp[-dk_0(1-c^2/v_1^2)^{1/2}]\sin(k_0 r - \omega t + \tan^{-1}\omega/\sigma)}{rH(v_p/v_1)(\sigma^2+\omega^2)^{1/2}[(v_1/c)(v_1/U)^2 d(U/v_1)/d\gamma]^{1/2}} \tag{51}$$

for $d(U/v_1)d\gamma > 0$.

A glance at the phase and group velocity curve in Fig. 9 shows that the approximation used in evaluating Eq. (48) fails at the times $t_m = r/U_{max}$ and $t = r/v_1$ corresponding respectively to the arrival of waves travelling with a maximum value of group velocity and waves for which $\gamma > \gamma_a$, where the phase and group velocity are constant.

For the maximum value of group velocity the method of stationary phase can still be used to evaluate Eq. (48) and gives (see Havelock[21]):

$$w_0 = \frac{(4/3)\sin(\pi/3)\Gamma(1/3)W(k_0)\exp[-dk_0(1-c^2/v_1^2)^{1/2}]\cos(k_0 r - \omega_0 t - \pi/4 + \tan^{-1}\omega/\sigma)}{r^{5/6}(1/6)^{1/3}(v_p/v_1)H^{1/2}(\sigma^2+\omega^2)^{1/2}[2\pi H^2(v_1/c)^2(v_1/U)^2 d^2(U/v_1)/d\gamma^2]^{1/3}} \tag{52}$$

In the region $\gamma_a < \gamma < \infty$ of constant phase and group velocity the method of stationary phase fails to evaluate the integral in Eq. (48). Waves propagated at a constant value of phase and group velocity are nondispersive, and the signal arriving at a time $t = r/v_1$ would have the analogous characteristics of a pulse transmitted through a high pass filter with a low frequency cutoff at $f_a = \gamma_a v_1/H$. However, the excitation function $W(k)$ is vanishingly small for all $f > f_a$, and has appreciable value only at $f \simeq f_a$. Consequently, the resultant signal at $t = r/v_1$ would have the characteristics of a pulse transmitted through a sharply tuned band pass filter with peak frequency at $f = f_a$.

[21] T. H. Havelock, "The Propagation of Disturbances in Dispersive Media," *Cambridge Tracts in Mathematical Physics*, No. 17, Cambridge University Press; 1914.

DISCUSSION OF THEORY

In the previous section the steady state solution, Eq. (25), was expressed as the sum of the residue of the integrand and two integrals along branch lines corresponding to branch points $k = \omega/v_1$ and $k = \omega/v_3$. The branch line integrals represent waves travelling with velocities v_3 and v_1 respectively and diminishing in amplitude with distance as r^{-2}. The residue contributes dispersive waves which predominate at large distance since they diminish only as $r^{-1/2}$. Equation (36) gives the functional relationship between phase velocity and frequency which characterizes the dispersion. Phase velocity is plotted as a function of the dimensionless parameter $\gamma = kH/2\pi = Hf/c$ in Fig. 9. Wave amplitudes for the steady state depend on frequency through the factor $W(k)$ given in Eqs. (39) through (40). A graph of $W(k)$ as a function of γ is presented in Fig. 10, for a source in the air. Interchanging the subscripts 1 and 3 in Eqs. (39) through (40) enables one to compute the corresponding amplitudes for a source in the water (Fig. 11).

Study of these curves for the steady state reveals that a peak amplitude exists for a point source in the air at a frequency f_a corresponding to the phase velocity $c = v_1$. For a point source in the water largest amplitudes are associated with low frequency waves. As the frequency (and phase velocity) increases, wave amplitudes decrease and abruptly drop to zero as the frequency f_a is approached.

Generalization of the steady state solutions for an impulsive point source leads to the group velocity curve presented in Fig. 9. At a distant point waves of a given frequency will arrive at a time corresponding to propagation at the group velocity associated with that frequency. In addition wave amplitudes are proportional to the inverse square root of the slope of the group velocity curve. Referring to Eqs. (50) through (51), one can obtain an amplitude factor for an impulsive point source

$$P(k_0) = \frac{2W(k_0)\exp[-dk_0(1 - c^2/v_1^2)^{1/2}]}{[(v_1/c)(v_1/U)^2 d(U/v_1)/d\gamma]^{1/2}} \tag{53}$$

from which wave amplitudes at large range can be obtained. Graphs of $P(k_0)$ have been computed from Eq. (48) and are presented in Figs. 12 and 13 for an air shot and water shot respectively, located at a distance $d = 5H$ from the ice sheet. With the aid of Figs. 9, 12, and 13, one can describe in a fairly complete manner the sequence of waves arriving at a distant point.

For an air shot the first waves to arrive appear at the time $t = r/2.2v_1$ corresponding to propagation at the maximum value of group velocity. These waves appear with large amplitudes and with a frequency close to f_a. As time progresses two wave trains arrive simultaneously corresponding to the two branches of the group velocity curve on either side of

the maximum. Waves propagated according to the left branch of the group velocity curve are dispersive and undergo a rapid reduction in amplitude as the frequency decreases from the value f_a. Waves propagated according to the steep branch of the group velocity curve to the right of the maximum appear as a constant frequency train continuing to the time $t = r/v_1$. The constant frequency waves would appear with relatively large amplitudes since their frequency f_a is close to the peak amplitude frequency. Thus the predominant disturbance appearing in an air shot would consist of a train of constant frequency waves beginning at the time $t = r/2.2v_1$ and ending abruptly at the time $t = r/v_1$. At this time an air wave would arrive corresponding to the flat portion of the group velocity curve. For reasons given earlier, it would have the characteristics of a pulse transmitted through a sharply tuned band pass filter with peak frequency at f_a.

For the case of a water shot the sequence of arrivals would be the same since the group velocity curve in Fig. 9 is still applicable. However, the amplitudes of the waves differ greatly (Fig. 13) in that the dispersive waves corresponding to the left branch of the group velocity curve are predominant. A water shot would therefore be characterized by a train of dispersive waves beginning at the time $t = r/2.2v_1$ with a frequency slightly less than f_a. As time increases, the frequency decreases and the amplitude increases. Although the steep portion of the group velocity curve still contributes constant frequency waves, these are now negligibly small. It is interesting to note that the portion of the group velocity curve to the left of the maximum is identical to that which would have been obtained had we neglected the air and it is this portion of the group velocity curve which is responsible for the predominant waves appearing in a water shot. Thus for frequencies less than f_a the dispersion and amplitudes of flexural waves from a water shot are unaffected by the air. It is only for an air shot that a constant frequency train of "air-coupled" flexural waves appears.

APPENDIX

APPLICATIONS OF AIR-COUPLED FLEXURAL WAVES

Air-coupled flexural waves can provide a simple means for determining the thickness of a floating ice sheet. If the elastic constants of the different types of floating ice (i.e., smooth ice, rough ice, lake ice, salt water ice, etc.) in a given area are known, one can obtain the value γ_a from a curve such as that given in Fig. 5. This leads to a simple numerical relationship between frequency and average ice thickness between shot point and detector. If the elastic constants are unknown, the observed value of f_a can be used to estimate the flexural rigidity of the ice sheet. Ordinary caps can provide sufficient energy to obtain average ice thickness over profiles of a few hundred feet to several thousand feet. Larger charges may be needed for larger distances.

Air-coupled flexural waves are particularly adaptable for use with radio monitored geophones parachuted from a plane.

Additional tests are needed to gauge the accuracy of measurements of ice thickness using air-coupled flexural vibrations. Present data suggest that thickness can be determined to within 10 percent, possibly better.

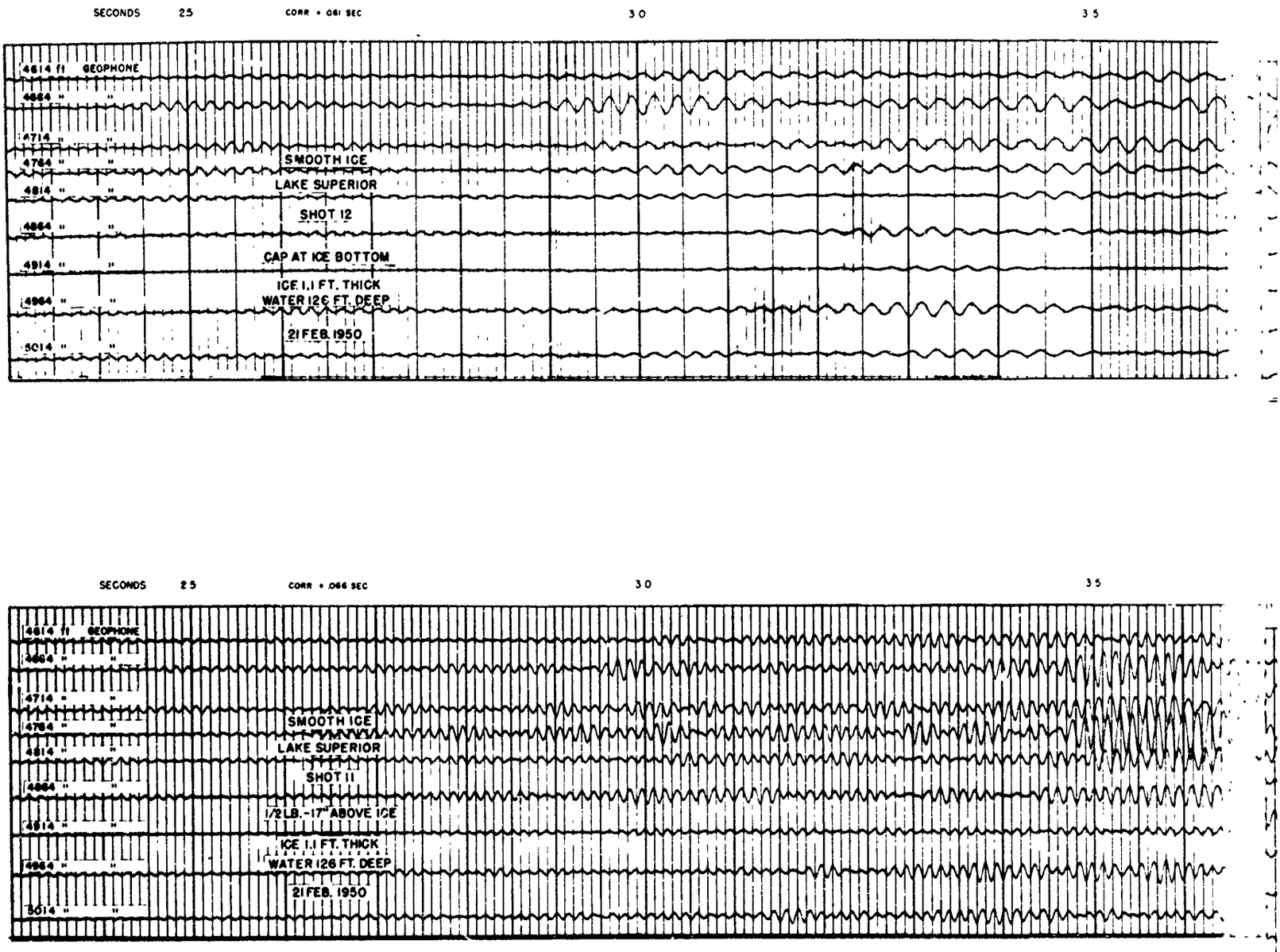

Fig. 1. Flexural waves from a water shot (a) and air-coupled flexural waves from an air shot (b) in smooth ice 1.1 ft thick.

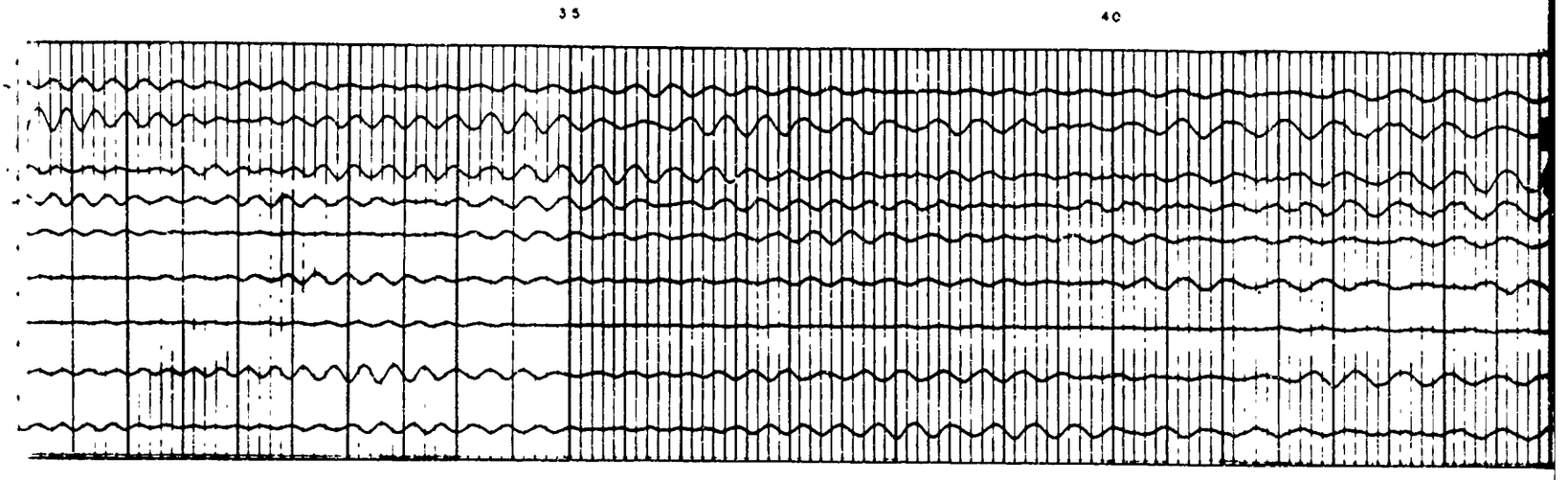

(a)

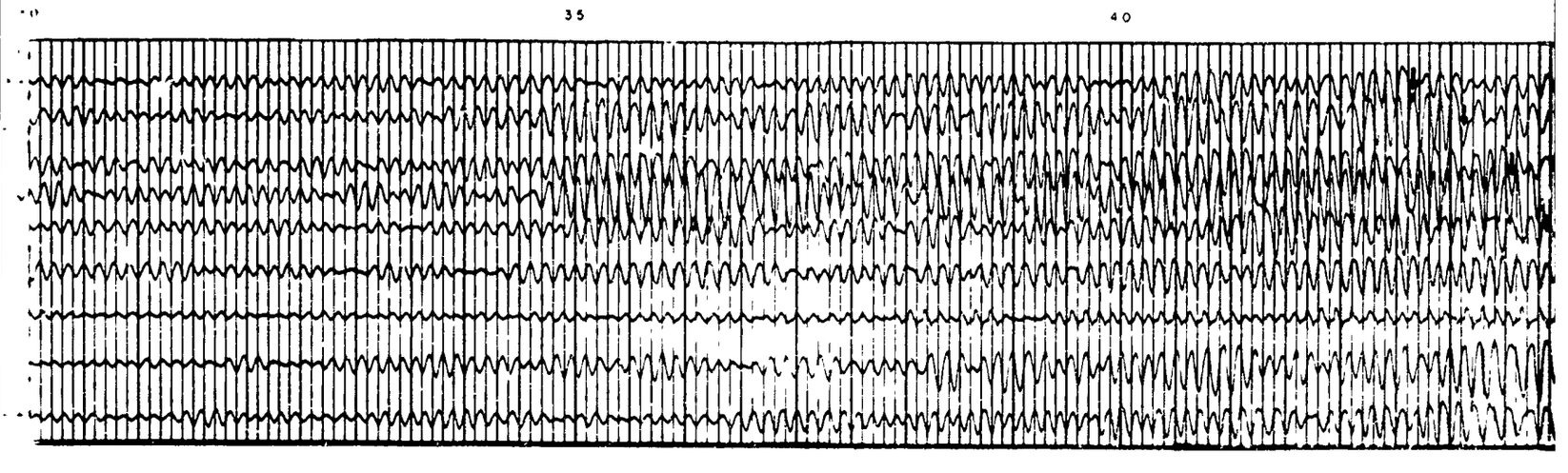

(b)

) and air-coupled flexural waves from an air shot

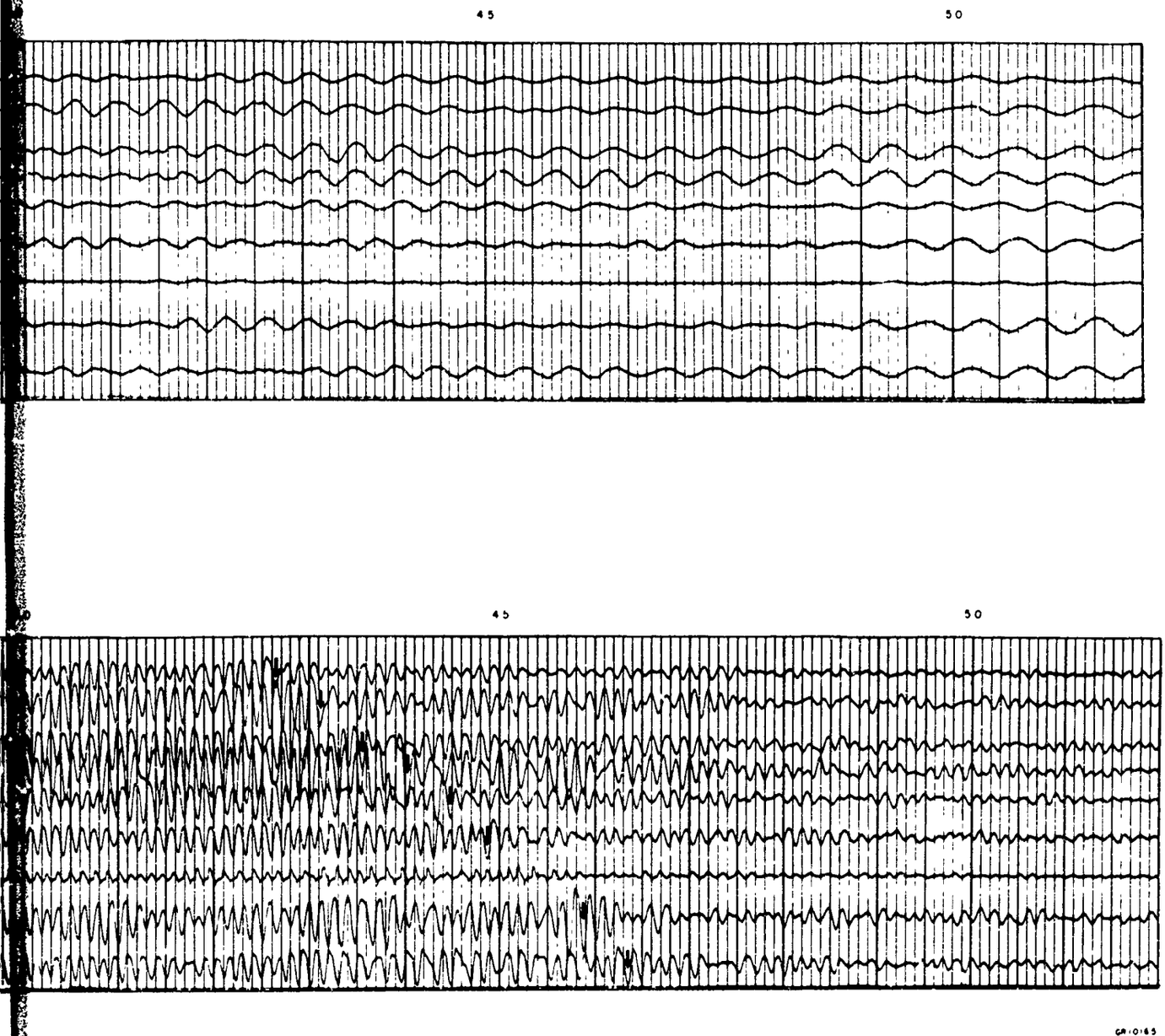

GR-10165

C

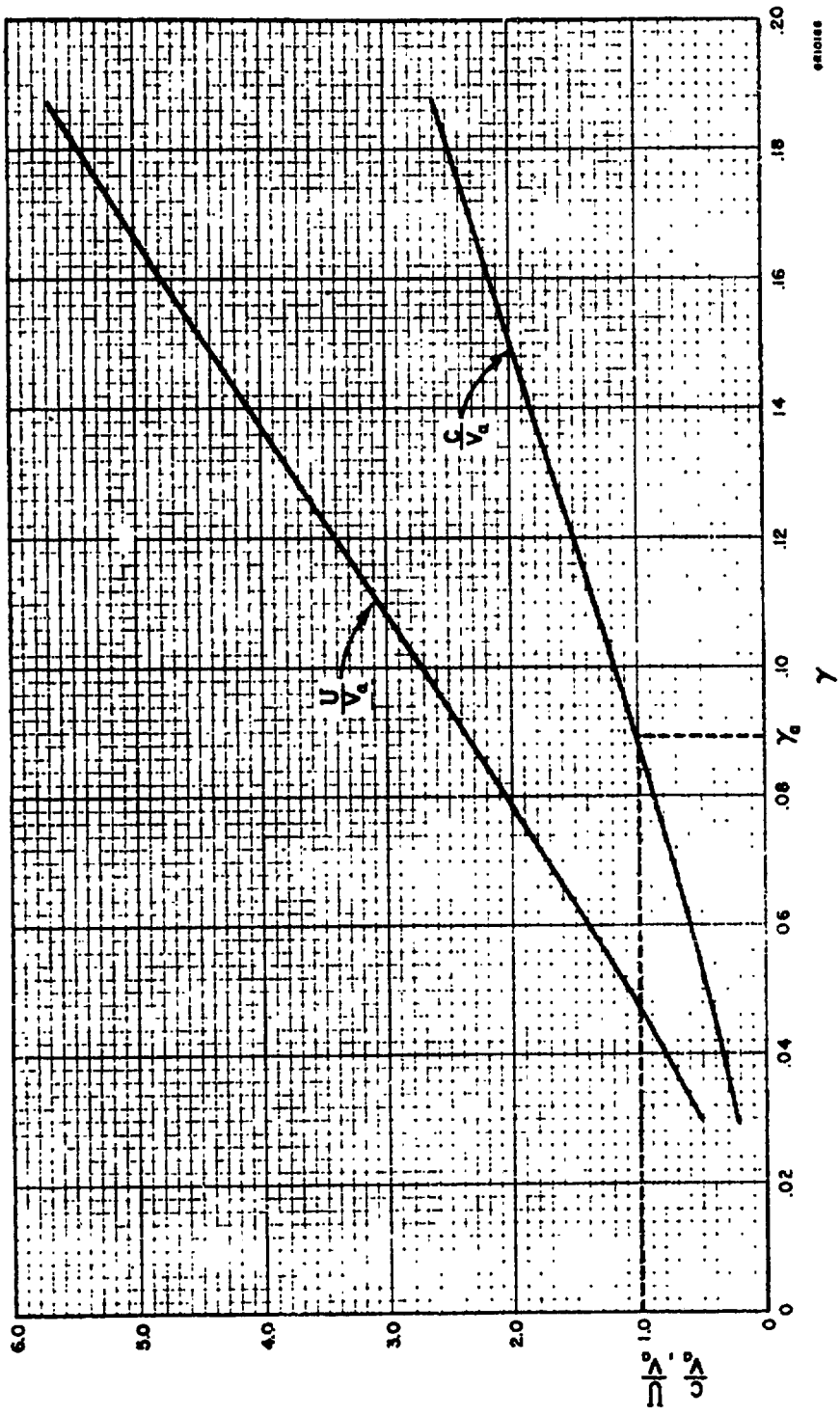

Fig. 2 Dimensionless phase and group velocity curves for flexural waves in a floating ice sheet.

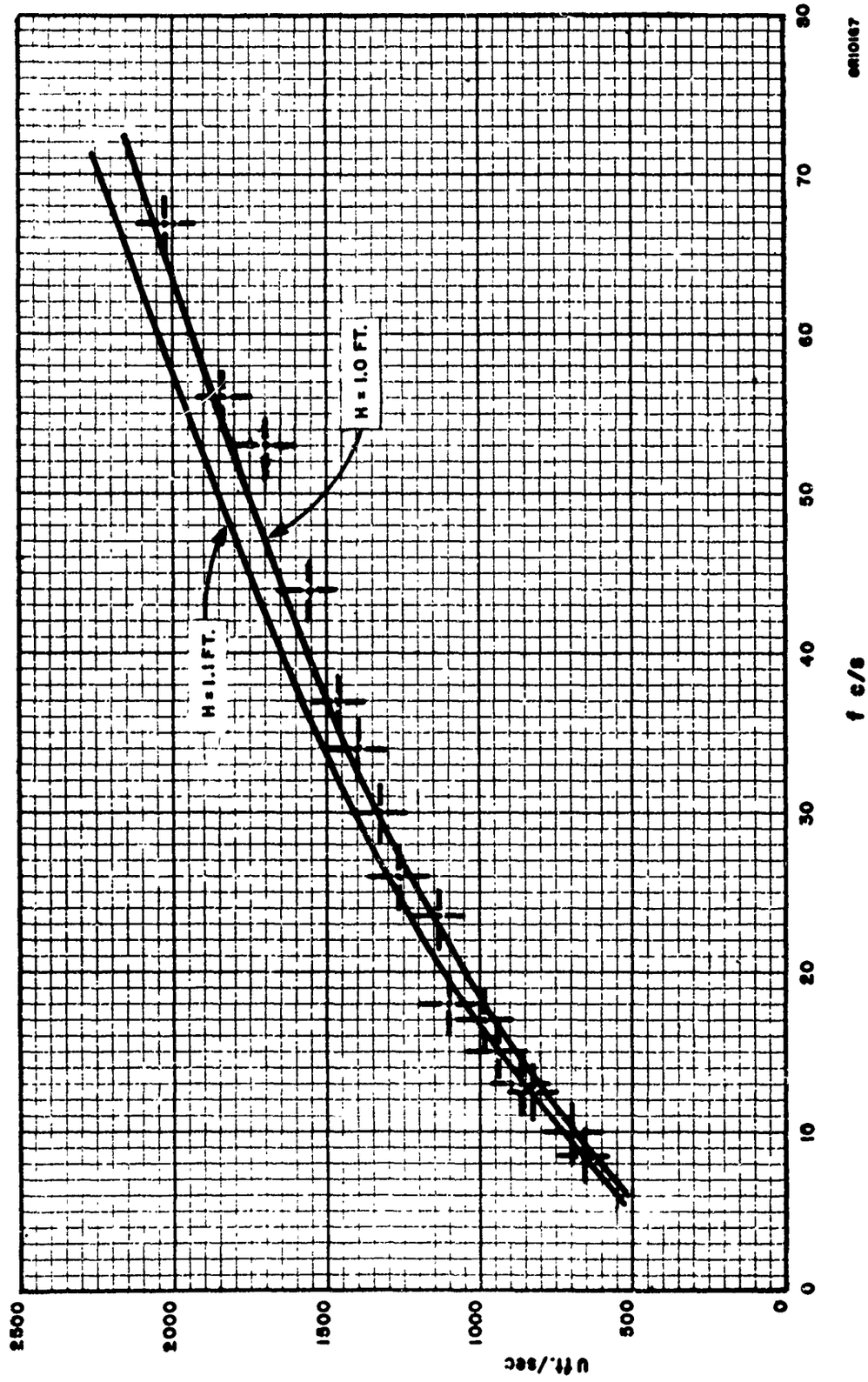

Fig. 3. Observed and theoretical dispersion of flexural waves.

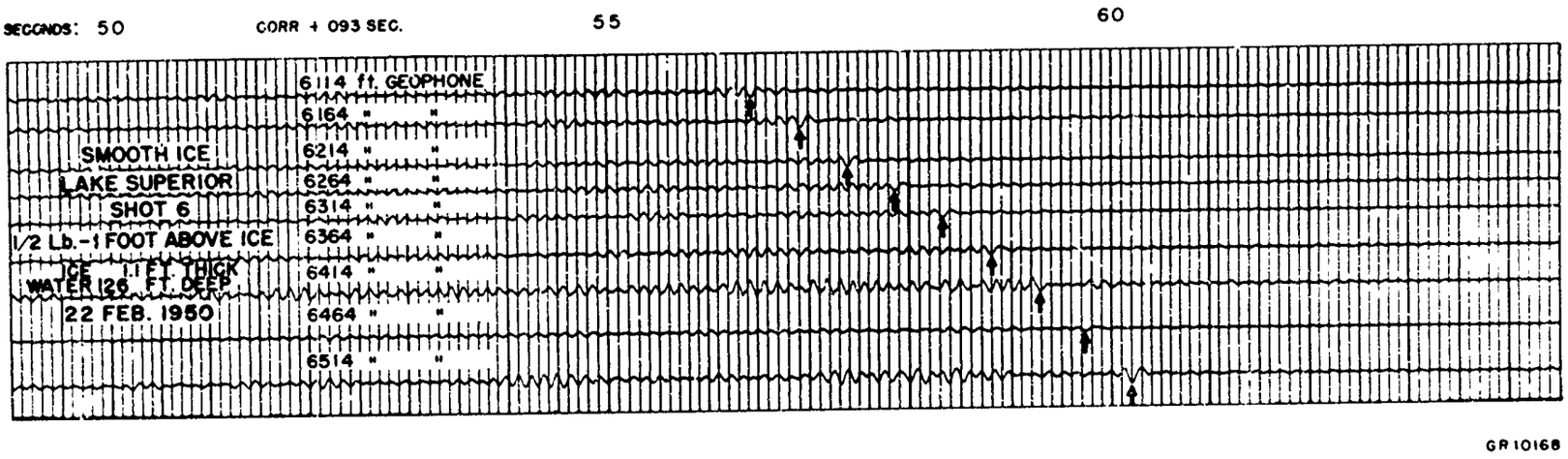

Fig. 4. Air-coupled flexural waves in smooth ice 1.1 ft thick recorded at reduced gain.

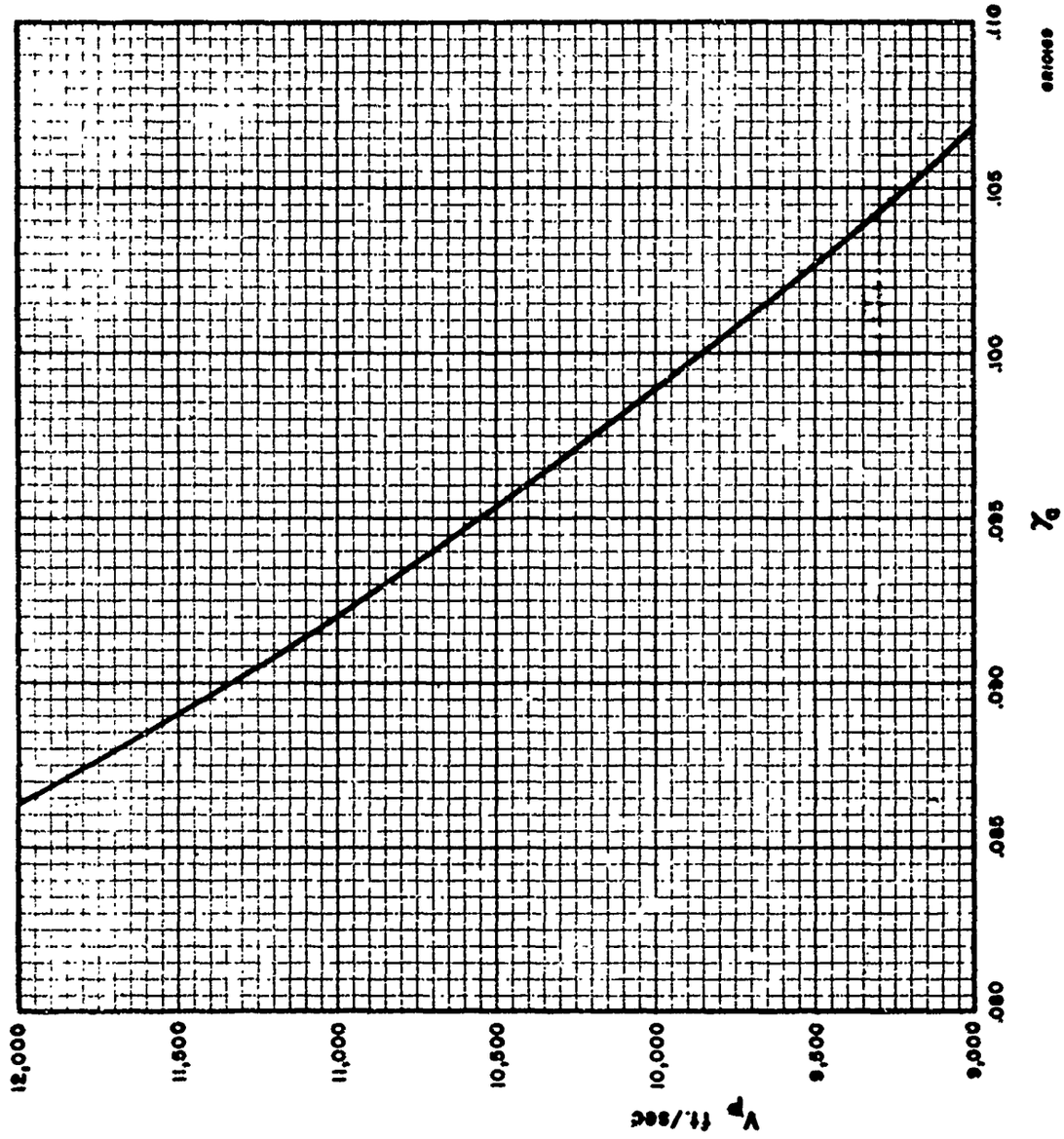

Fig. 5. Frequency parameter γ_e plotted as a function of longitudinal wave velocity.

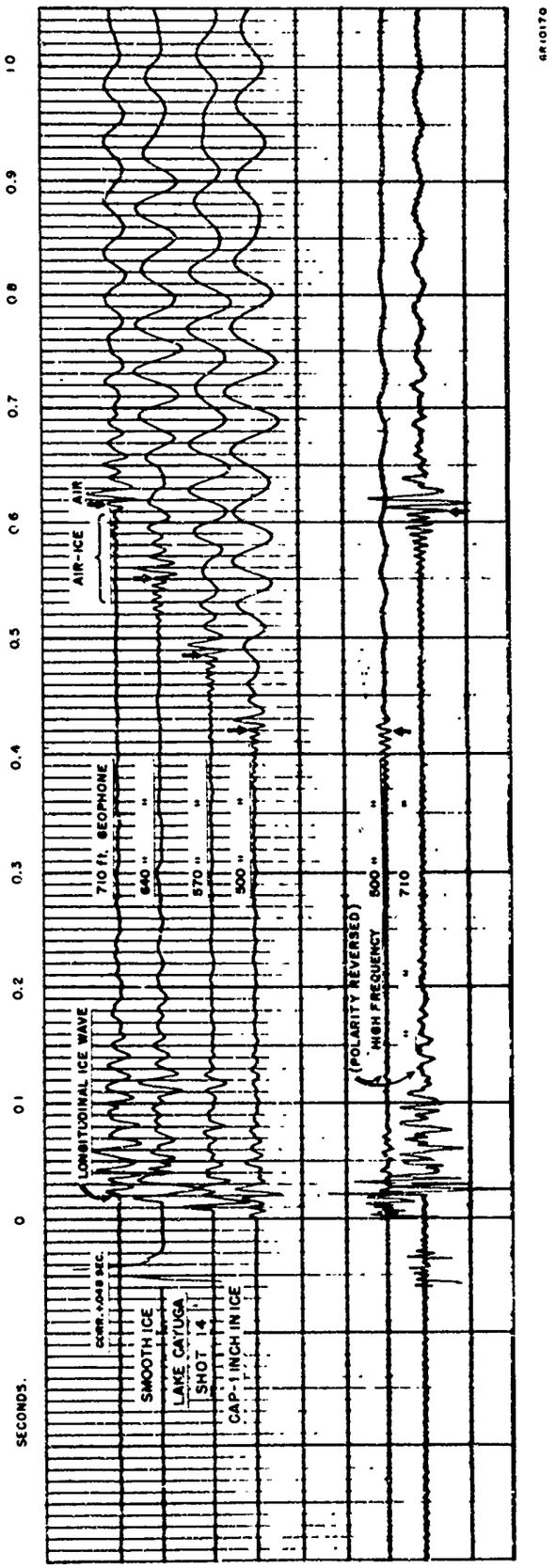

Fig. 6. Air-coupled flexural waves in smooth ice .66 ft thick.

Fig. 7. Air-coupled flexural waves in rough ice averaging 1.7 ft in thickness.

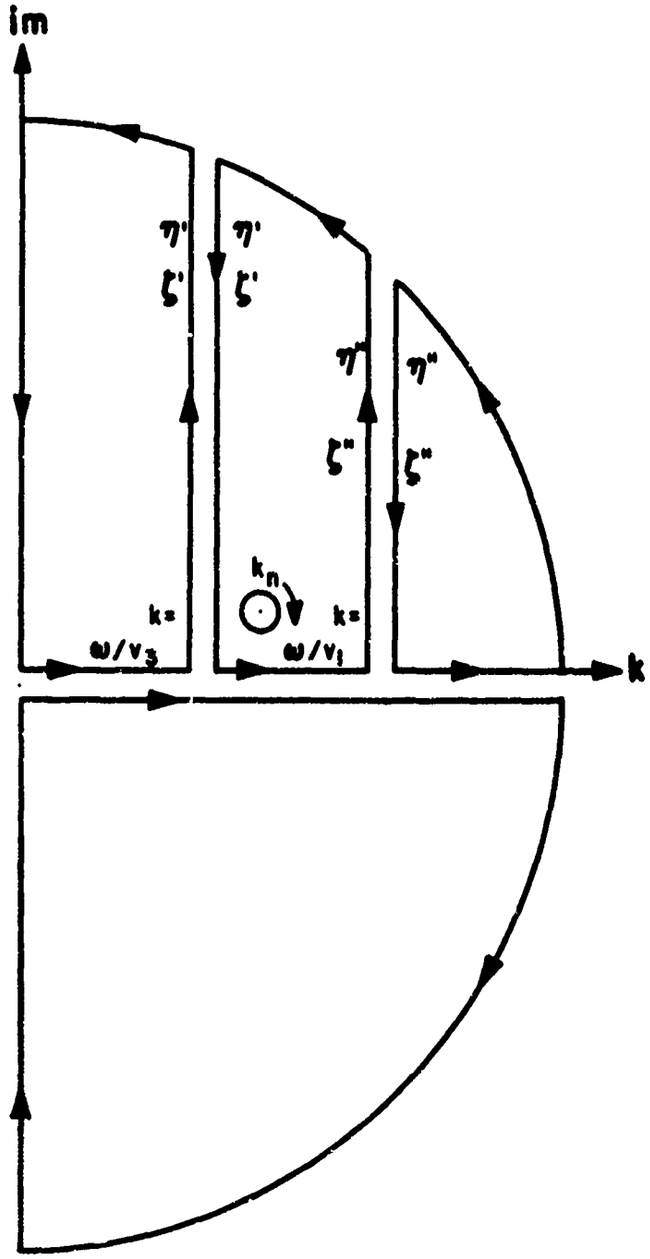

ORIGINAL

Fig. 8. Integration paths in the complex k plane.

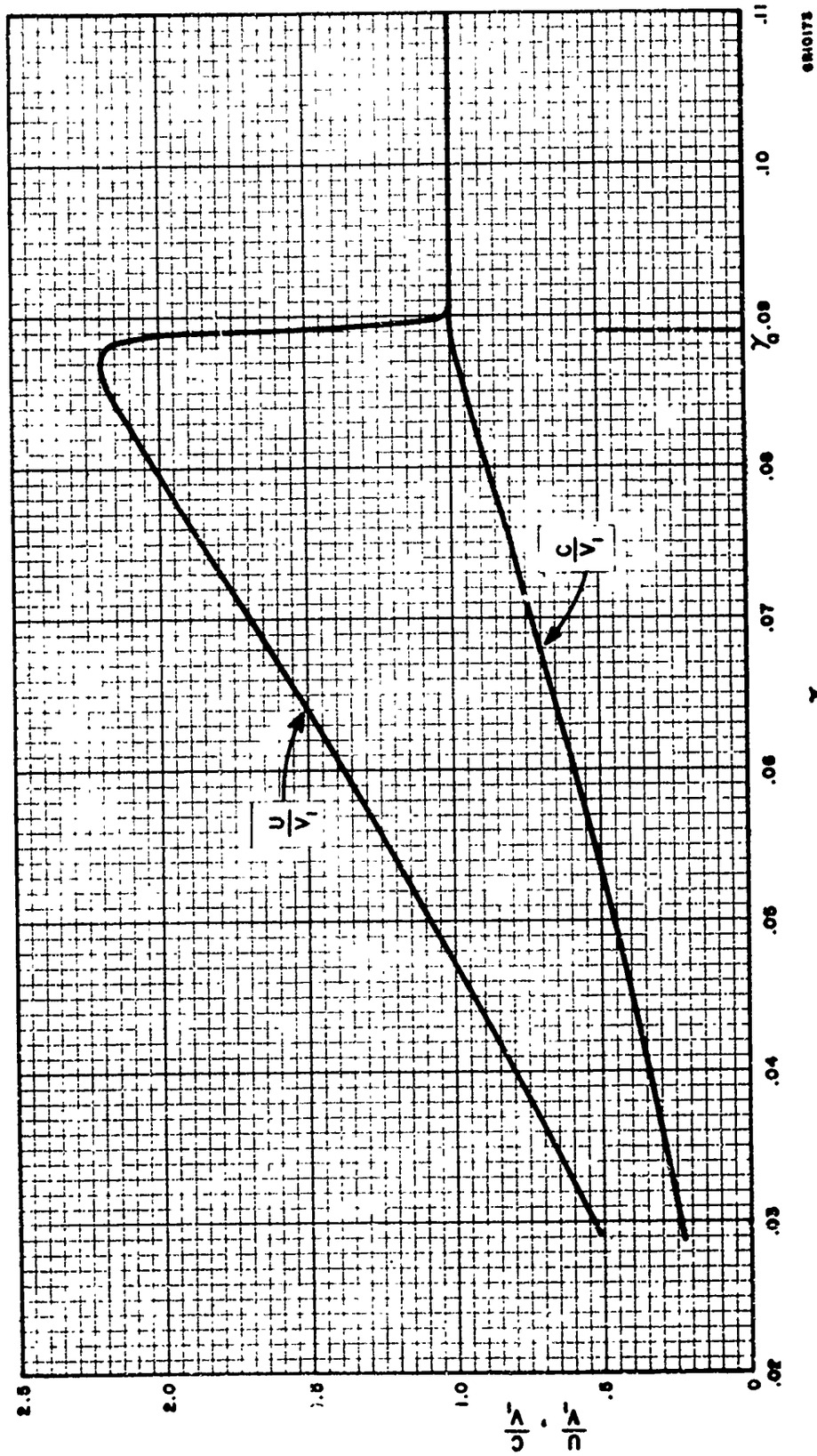

Fig. 9. Dimensionless phase velocity (c/v_1) and group velocity (U/v_1) curves.

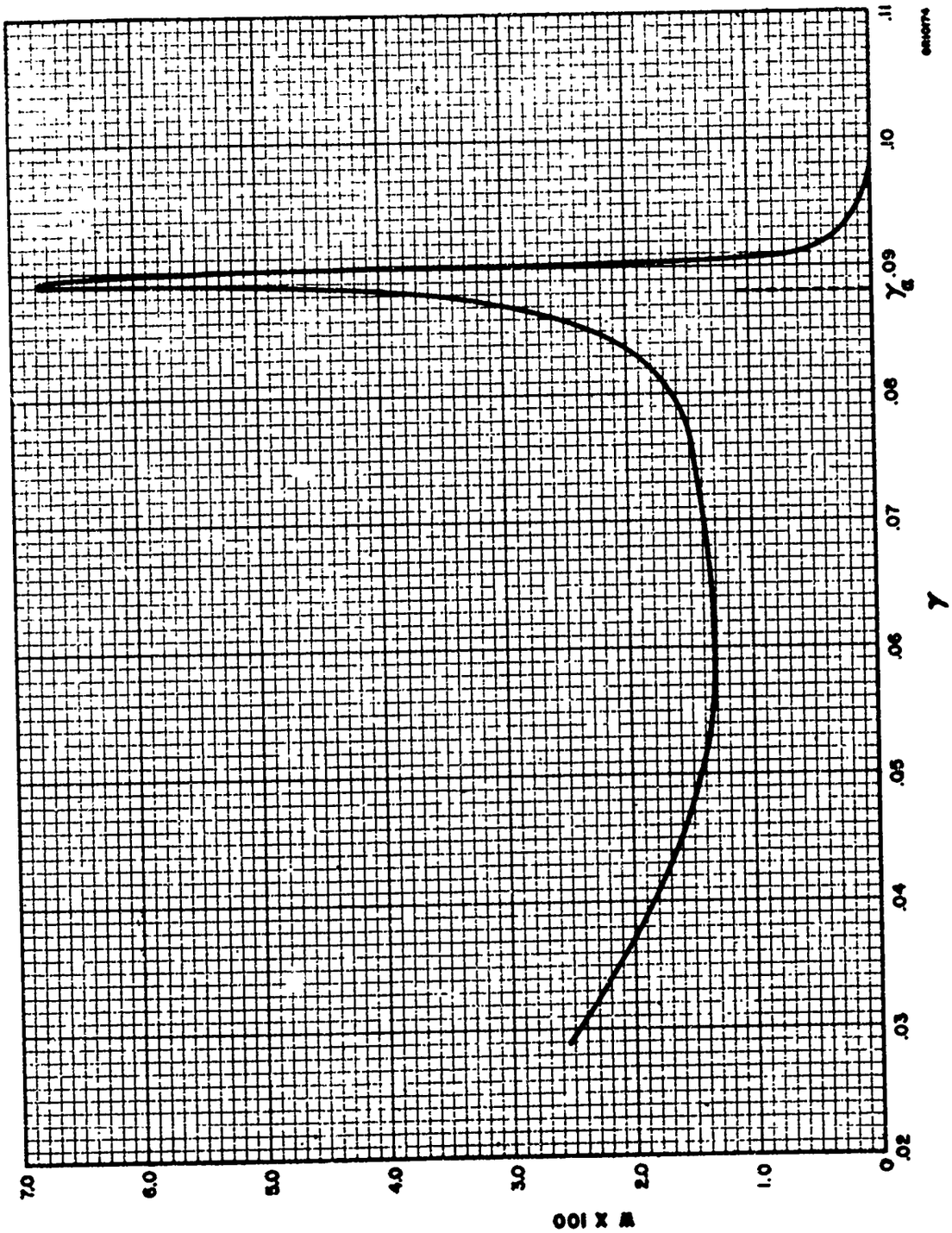

Fig. 10. Steady state amplitude function for an air source.

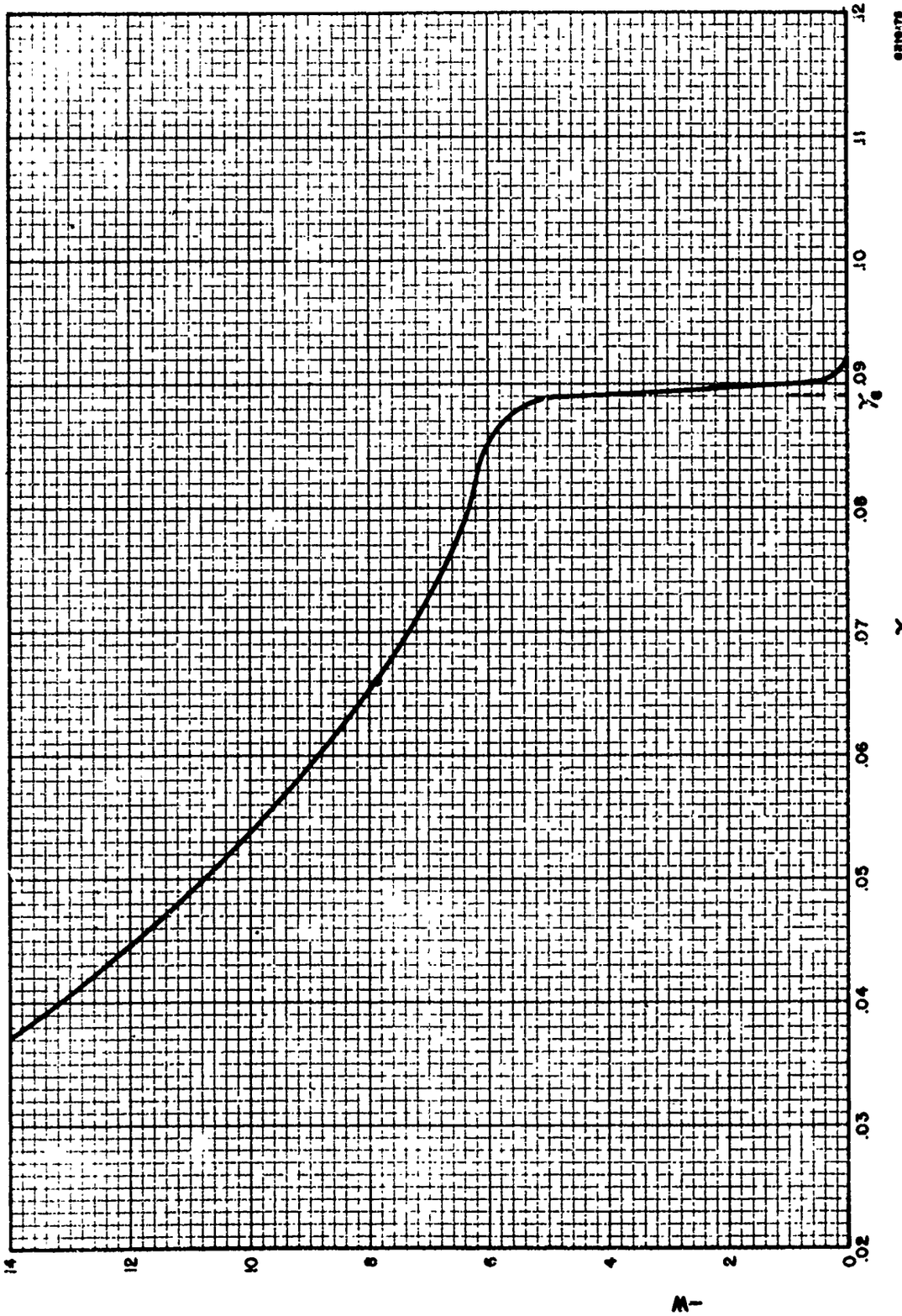

Fig. 11. Steady state amplitude function for a water source.

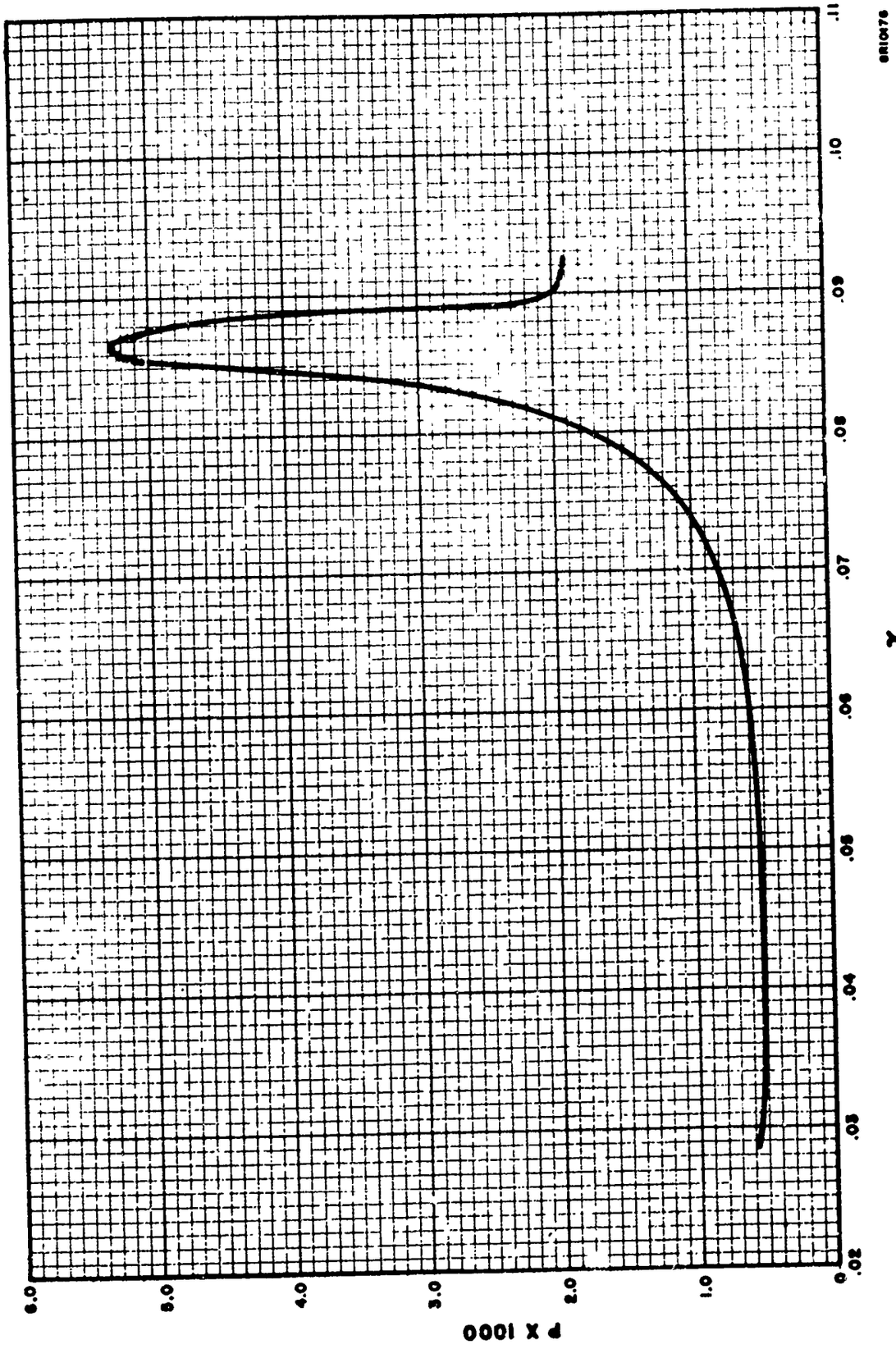

Fig. 12. Amplitude function for an air shot at $d = 5H$.

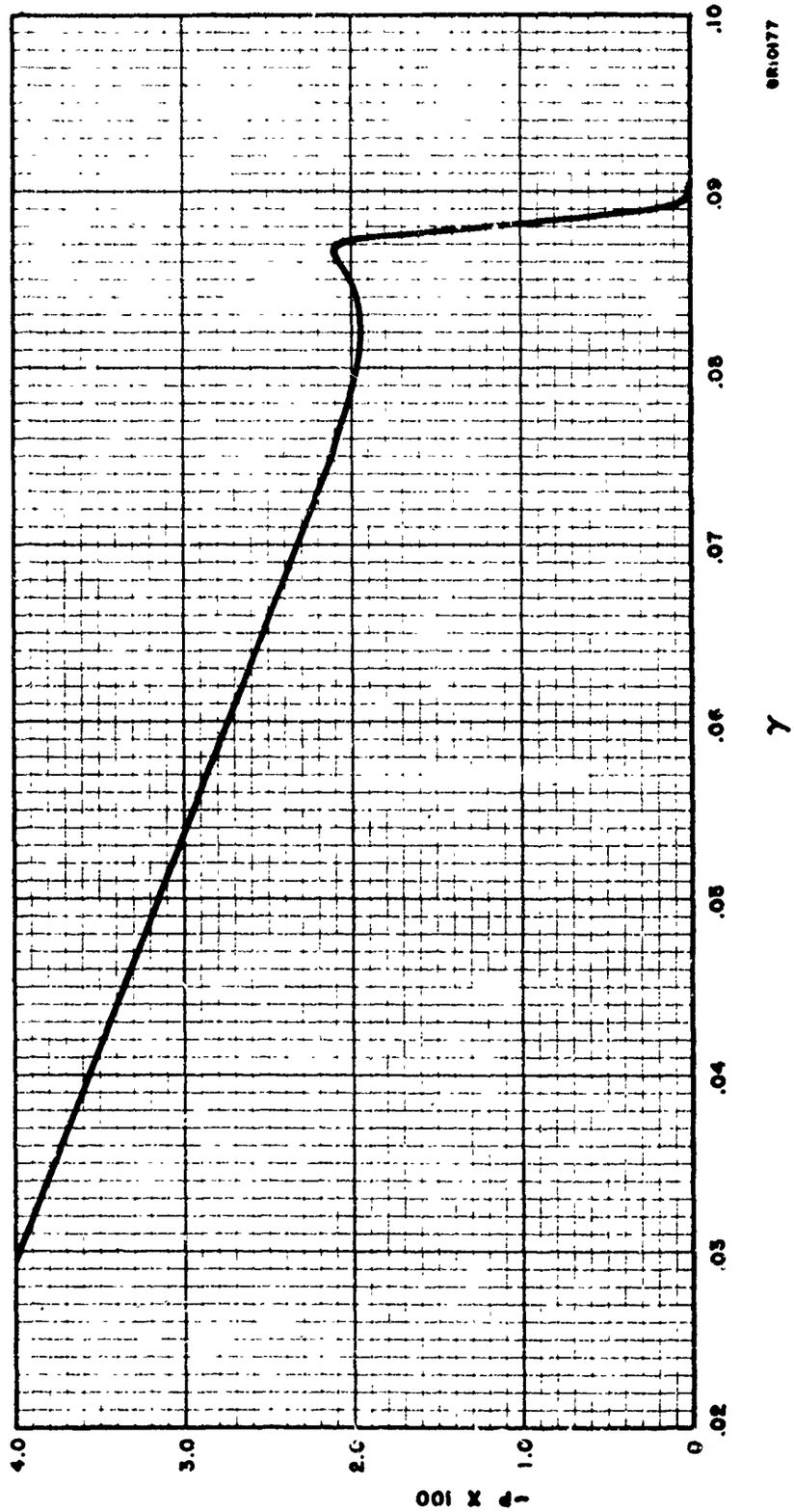

Fig. 13. Amplitude function for a water shot at $d = 5H$.

GEOPHYSICAL RESEARCH PAPERS

No. 1. Isotropic and Non-Isotropic Turbulence in the Atmospheric Surface Layer, Heinz Lettau, Geophysical Research Directorate, December 1949.

No. 2. (Classified).

No. 3. Diffraction Effects in the Propagation of Compressional Waves in the Atmosphere, Norman A. Haskell, Geophysical Research Directorate, March 1950.

No. 4. Evaluation of Results of Joint Air Force - Weather Bureau Cloud Seeding Trials Conducted During Winter and Spring 1949, Charles E. Anderson, Geophysical Research Directorate, May 1950.

No. 5. Investigation of Stratosphere Winds and Temperatures from Acoustical Propagation Studies, A. P. Crary, Geophysical Research Directorate, June 1950.